

# Anomalous Magnetoresistance in Pb-doped $\text{Bi}_2\text{Sr}_2\text{Co}_2\text{O}_y$ Single Crystals

X. G. Luo, X. H. Chen\*, G. Y. Wang, C. H. Wang, X. Li, W. J. Miao, G. Wu, and Y. M. Xiong  
Hefei National Laboratory for Physical Science at Microscale and Department of Physics,  
University of Science and Technology of China, Hefei,  
Anhui 230026, People's Republic of China

(Dated: April 11, 2017)

Magnetoresistance (MR) of the  $\text{Bi}_{2-x}\text{Pb}_x\text{Sr}_2\text{Co}_2\text{O}_y$  ( $x=0, 0.3, 0.4$ ) single crystals is investigated systematically. A nonmonotonic variation of the isothermal in-plane and out-of-plane MR with the field is observed. The out-of-plane MR is positive in high temperatures and increases with decreasing  $T$ , and exhibits a pronounced hump, and changes the sign from positive to negative at a certain temperature. These results strongly suggest that the observed MR consists of two contributions: one *negative* and one *positive* component. The isothermal MR in high magnetic fields follows a  $H^2$  law. While the negative contribution comes from spin scattering of carriers by localized-magnetic-moments based on the Khosla-Fischer model.

PACS numbers: 75.47.-m, 71.30.+h, 71.27.+a

## I. INTRODUCTION

The triangular cobalt oxides attracted a great deal of interest for the large thermoelectric power (TP) with low resistivity and low thermal conductivity (thus the large thermoelectric figure of merit  $ZT = S^2T/\rho\kappa$ ) for the application reasons. A lot of efforts has focused on the enhancement of the figure of merit.<sup>1,2,3</sup> One important aspect for such effort is to make out why the metallic oxides with triangular  $\text{CoO}_2$  layers have such unusually large TP comparing to the conventional metal. Therefore, the work on understanding the fundamental properties of this systems becomes especially significant.

A number of results has been obtained on the transport and magnetic properties of the triangular cobaltites, such as Curie-Weiss susceptibility and temperature-dependent Hall coefficient and anomalous magnetoresistance.<sup>1,4,5,6,7,8</sup> Recently, superconductivity was found in one of the promising thermoelectric triangular cobaltite  $\text{Na}_x\text{CoO}_2$  with  $x=0.35$  by intercalating water molecules into between the  $\text{Na}^+$  and  $\text{CoO}_2$  layers.<sup>9</sup> Later, Foo et al.<sup>10</sup> observed an insulating resistivity below 50 K in the composition of  $x=0.5$ , which is considered to be related to the strong coupling of the holes and the long-range ordered  $\text{Na}^+$  ions. The strong magnetic field dependence of TP in  $\text{Na}_x\text{CoO}_2$  provides an unambiguous evidence of strong electron-electron correlation in the thermoelectric cobalt oxides.<sup>11</sup> The large TP with metallic resistivity, superconductivity, charge ordering existing with various  $x$ , displays a complicated and profuse electronic state in  $\text{Na}_x\text{CoO}_2$ . This has inspired numerous theoretical and experimental studies on the triangular cobalt oxides.

In this paper, we present new results on the magnetoresistance (MR) of  $\text{Bi}_{2-x}\text{Pb}_x\text{Sr}_2\text{Co}_2\text{O}_y$  ( $x=0.0-0.4$ ) ((Bi,Pb)-Sr-Co-O) single crystals. It has been reported that there exhibits large *negative* MR in  $\text{Ca}_3\text{Co}_4\text{O}_9$ ,  $\text{Bi}_{2-x}\text{Pb}_x\text{Sr}_2\text{Co}_2\text{O}_y$  and  $[\text{Bi}_{1.7}\text{Co}_{0.3}\text{Ca}_2\text{O}_4]^{\text{RS}}[\text{CoO}_2]_{1.67}$  (Bi-Ca-Co-O),

$[\text{Pb}_{0.7}\text{A}_{0.4}\text{Sr}_{1.9}\text{O}_{1.9}\text{O}_3]^{\text{RS}}[\text{CoO}_2]_{1.8}$  ( $\text{A}=\text{Hg}, \text{Co}$ )<sup>1,3,4,5,12</sup> while *positive* MR in  $\text{Tl}_{0.4}[\text{Sr}_{0.9}\text{O}]_{1.12}\text{CoO}_2$ ,  $[\text{Bi}_2\text{Ba}_{1.8}\text{Co}_{0.2}\text{O}_4]^{\text{RS}}[\text{CoO}_2]_2$  (Bi-Ba-Co-O) and  $\text{Na}_{0.75}\text{CoO}_2$ .<sup>6,7,8</sup> Very recently, a magnetic-field-induced insulator-to-metal transition was observed by us in oxygen-annealed  $\text{Ca}_3\text{Co}_4\text{O}_9$ .<sup>12</sup> Large negative MR is ascribed to suppression of spin scattering.<sup>1,3,4,5</sup> The positive  $H^2$ -dependence of MR in  $\text{Na}_{0.75}\text{CoO}_2$  is attributed to conventional orbital motion of carriers,<sup>8</sup> while linear positive MR is interpreted in an opening of pseudogap.<sup>7</sup> Up to now, the anomalous MR is not well understood entirely yet. Further detailed investigation is required to describe the physical nature of these triangular cobaltites. For the easy control of doping level, Pb-doped  $\text{Bi}_2\text{Sr}_2\text{Co}_2\text{O}_y$  single crystals are chosen to be studied systemically. The Pb-free sample, with the exact formula as  $[\text{Bi}_{0.86}\text{SrO}_2]_2^{\text{RS}}[\text{CoO}_2]_{1.82}$ ,<sup>13</sup> is paramagnetic down to 2 K.<sup>5,14</sup> With doping by Pb, weak ferromagnetism is induced, which is considered to originate from a canted-antiferromagnetism or to coexist with spin-glass.<sup>5,15</sup> The coexistence of ferromagnetic and antiferromagnetic interaction makes this system intriguing. In this paper, the magnetoresistance, measured in in-plane and out-of-plane configurations with the fields up to 13.5 T, is observed to exhibit nonmonotonic field-dependent behavior. The MR shows a complicated dependence of the field and temperature. Its magnitude is enhanced initially with increasing  $H$ , and reaches a maximum at a certain field. The  $T$  dependence of the out-of-plane MR is positive in high temperatures, and shows a pronounced hump with decreasing  $T$ . These results suggest the MR comes from the contribution of negative and positive components, which is strongly dependent of temperature and field.

## II. EXPERIMENT

The  $\text{Bi}_{2-x}\text{Pb}_x\text{Sr}_2\text{Co}_2\text{O}_y$  ( $x=0.0, 0.3, 0.4$ ) single crystals were grown by a self-flux method. High-purity

$\text{Bi}_2\text{O}_3$ ,  $\text{PbO}$ ,  $\text{SrCO}_3$  and  $\text{Co}_3\text{O}_4$  were mixed with a nominal mole ratio of  $\text{Bi:Pb:Sr:Co}=2-x:x:2:2$  ( $x=0.5$  and  $0.6$ ) and preheated at  $800^\circ\text{C}$  for 24 h. Additional  $\text{Bi}_2\text{O}_3$  as the flux was mixed with the obtained precursors carefully. The mixture was melt at  $1050^\circ\text{C}$  for 2 h, and followed a slow cooling procedure with a cooling rate of  $4\text{-}5^\circ\text{C/h}$  to  $800^\circ\text{C}$ , then cooled by furnace. Platelike crystals were easily cleaved from the melt. The actual composition of  $0.3$  and  $0.4$  was determined by inductively coupled plasmas (ICP) atomic emission spectroscopy for the nominal composition of  $x=0.5$  and  $0.6$ , respectively. The measurements of in-plane and out-of-plane resistivity with a configuration described in ref. 16 were performed using the standard ac four-probe method. The magnetic field was supplied by a superconducting magnet system (Oxford Instruments).

### III. EXPERIMENTAL RESULTS AND DISCUSSION

#### A. Transport properties

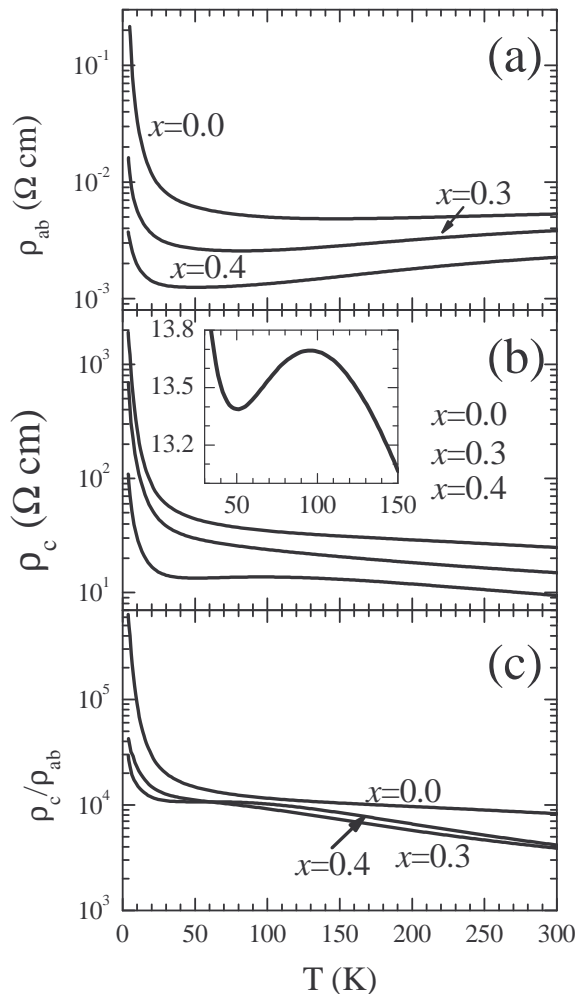


FIG. 1: The temperature dependence of in-plane (a), out-of-plane (b) resistivity and the anisotropy  $\rho_c/\rho_{ab}$  (c).

Figure 1(a) shows the temperature dependence of the in-plane resistivity ( $\rho_{ab}(T)$ ) of samples  $x=0.0$ ,  $0.3$ , and  $0.4$ . The crystals show metallic behavior in high temperatures.  $\rho_{ab}(T)$  exhibits a minimum at  $140\text{ K}$  for  $x=0.0$ ,  $70\text{ K}$  for  $x=0.3$ , and  $45\text{ K}$  for  $x=0.4$ , respectively. Below this temperature the crystals show a diverging resistivity. The resistivity and the temperature corresponding to the resistivity minimum decrease with increasing the content of the Pb substitution for Bi. The ratio  $\rho_{ab}(T=4\text{K})/\rho_{ab}(T=300\text{K})$  decreases also with enhancing the doping level of Pb. These indicate that the Pb doping induces holes into the system. These results are consistent with the previous report.<sup>5</sup> Figure 1(b) shows the temperature dependence of the out-of-plane resistivity ( $\rho_c(T)$ ) of the samples. For the samples with  $x=0.0$  and  $x=0.3$ ,  $\rho_c(T)$  shows insulator-like behavior in the whole temperature range. It increases slightly above about  $50\text{ K}$  and enhances suddenly below  $50\text{ K}$  with decreasing temperature. For the sample with  $x=0.4$ ,  $\rho_c(T)$  shows an insulator-like behavior above  $100\text{ K}$  and below  $100\text{ K}$  it shows a metallic behavior ( $d\rho_c/dT>0$ ). With further decreasing temperature down to  $30\text{ K}$ ,  $\rho_c(T)$  shows a reentrant insulating behavior and increases sharply with decreasing temperature. It shows a broad maximum at  $T_M \approx 100\text{ K}$ . Such a broad maximum is very similar to that observed in  $(\text{Bi}_{0.5}\text{Pb}_{0.5})_2\text{Ba}_3\text{Co}_2\text{O}_y$  ( $T_M \approx 200\text{ K}$ ) and  $\text{NaCoO}_2$  ( $T_M \approx 180\text{ K}$ ), where it is thought to be an incoherent-coherent resistivity transition.<sup>17</sup> This transition was considered as a crossover in the number of effective dimension from two to three.<sup>17</sup> The diverging resistivity in the low temperatures has been attributed to the decrease of the effective carrier number  $n$  due to a pseudogap formation below  $30\text{-}50\text{ K}$ .<sup>18</sup> In addition, the Hall coefficient was reported to exhibit a sudden enhancement,<sup>5,19</sup> suggesting a reduction of  $n$  in low temperatures. Another point of view is that the resistivity upturn and the sudden enhancement of Hall coefficient below  $50\text{ K}$  are associated with the magnetic ordering in low  $T$ .<sup>6</sup>

Figure 1(c) shows the temperature dependence of the anisotropy  $\rho_c/\rho_{ab}$  for the three samples. The three samples show close values of the anisotropy. The anisotropy shows a weak temperature dependence above  $50\text{ K}$  for the samples. While the anisotropy increases sharply below  $30\text{ K}$ . It is addressed that the anisotropy for the sample  $x=0.4$  saturates below  $100\text{ K}$ , which coincides with the "incoherent-coherent" transition temperature. The temperature-independent anisotropy between  $100$  and  $30\text{ K}$  and the peak in  $\rho_c(T)$  for  $x=0.4$  sample give evidence for existence of the dimensional crossover from two to three. In order to make clear the physics of the diverging resistivity and "incoherent-coherent" transition, it requires angle-resolved photoemission to determine the electronic structure.

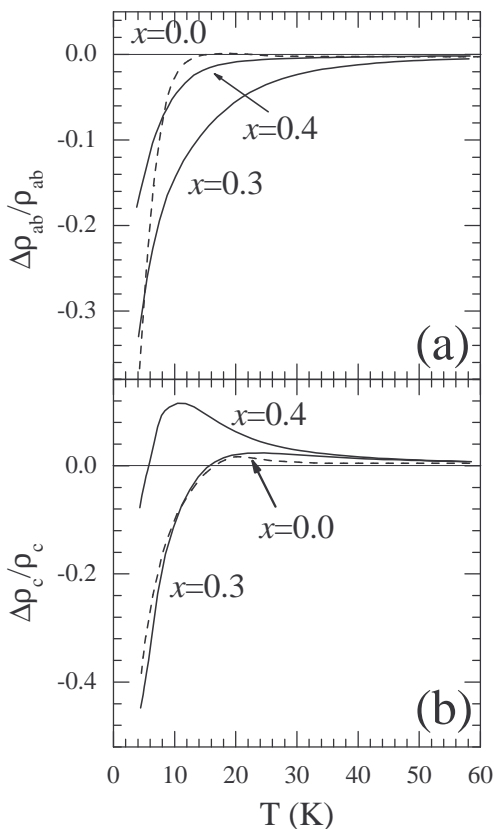


FIG. 2: The in-plane (a) and out-of-plane (b) magnetoresistance as a function of temperature at 13.5 T for the two samples. The field is applied along c-axis.

### B. Magnetoresistance

Figure 2 shows the evolution of  $\Delta\rho_{ab}/\rho_{ab}$  and  $\Delta\rho_c/\rho_c$  ( $\Delta\rho/\rho = ((\rho(H) - \rho(0))/\rho(0))$ ) with varying temperature at the field of 13.5 T. Above 12 K, the in-plane MR for  $x=0.0$  is very small and negative, and its magnitude increases sharply below 12 K with decreasing temperature. The negative MR reaches 37% at 4 K. The in-plane MR is negative and its magnitude monotonously increases with decreasing temperature, and reaches 33%, and 18% at 4 K for 0.3 and 0.4 sample, respectively. However, the out-of-plane MR shows anomalous features compared to the in-plane MR. The out-of-plane MR is positive in high temperatures for the samples. The MR first increases with decreasing temperature, and exhibits a broad hump. With further decreasing temperature, the MR changes the sign from positive to negative, and its magnitude begins to increase sharply.

In order to understand the anomalous behavior in out-of-plane MR, it was systematically studied in the different magnetic fields. The out-of-plane MR for the samples with  $x=0.3$  and 0.4 as a function of temperature at various magnetic fields is shown in Fig. 3. The MR is positive in high temperatures as observed in Fig.2, and increases monotonically with increasing magnetic field.

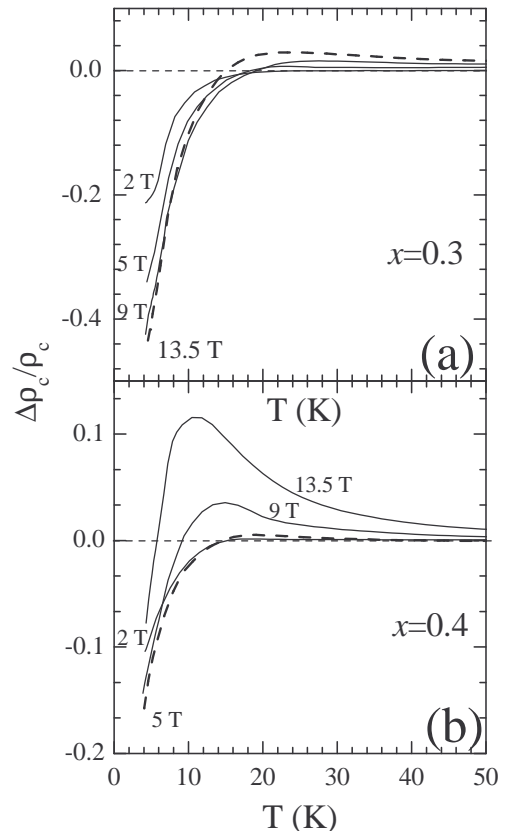


FIG. 3: The out-of-plane magnetoresistance as a function of temperature at various magnetic fields for the sample  $x=0.3$  (a)  $x=0.4$  (b). The field is applied along c-axis.

Broad humps of the positive MR can be observed at all magnetic fields for the two samples. The position of the humps shifts to lower temperature with enhancing magnetic field. With further decreasing  $T$ , the MR becomes negative in low temperatures. The temperature for the MR passing through zero decreases monotonously with increasing the field. The negative MR exhibits complex behavior at various fields. The magnitude of MR for  $x=0.3$  varies with field monotonically at 4 K, while exhibits maximum at 9 T as  $T$  is in the temperature range from 8 K to 18 K. The magnitude of MR for the  $x=0.4$  reaches maximum around 5 T at 4 K. These results suggests that the observed MR comes from two contributions, i.e. one negative and one positive contribution to the total MR. In high temperatures, the positive component is predominant, while the negative component grows more rapidly than the positive one with decreasing  $T$  and MR has a negative value in low temperatures.

In order to clearly understand the complicated behavior shown in Fig.3, isothermal MR is studied by sweeping the fields up to 13.5 T at different temperatures. Figure 4 shows the isothermal in-plane MR at 5, 15 and 40 K for the samples with  $x=0.0$ , 0.3, and 0.4. There are some salient features of the MR. (I) The MR at 40 K and 15 K for the crystal with  $x=0.0$  first increases

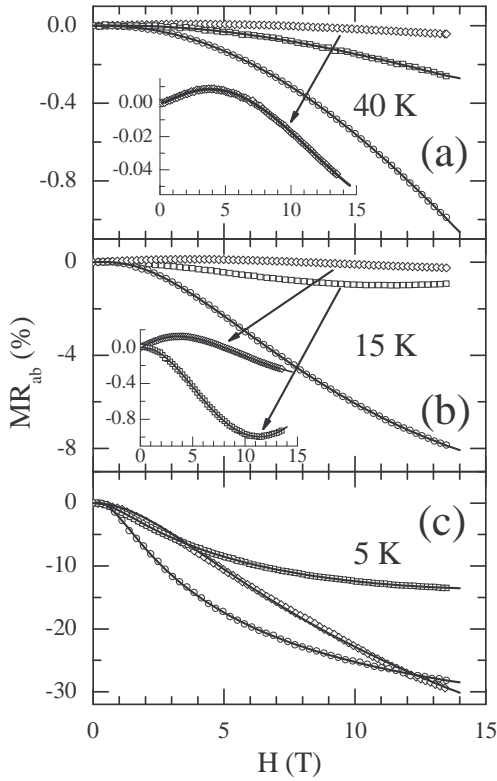


FIG. 4: The isothermal in-plane magnetoresistance as function of magnetic field at 40 K, 15 K, and 5 K for the samples with  $x=0.0$  ( $\diamond$ ),  $x=0.3$  ( $\circ$ ) and  $x=0.4$  ( $\square$ ), where  $MR=[\rho(H) - \rho(0)]/\rho(0) \times 100\%$ , the subindex ab is referred to the in-plane case. The solid lines are the data fitted by using Eq. (1). The field is applied along c-axis.

with increasing field, and reaches a maximum at 4 T (for both of the temperatures), then decreases monotonically. Such a MR has not been observed in the misfit-layered cobaltites. (II) All the other MR curves are negative, with the magnitude increasing with decreasing temperature. The magnitude of these MR increases monotonically with increasing magnetic field except that at 15 K in the sample  $x=0.4$ . (III) The magnitude of the MR at 15 K for  $x=0.4$  first increases with increasing magnetic field, and reaches a maximum ( $\sim 10\%$ ) at 11.4 T, then decreases with further increasing field (see the inset in Fig. 4(b)). It suggests the presence of a positive contribution in addition to the negative MR in this case. Such an anomalous MR has not been observed in triangular cobaltites previously. Only large monotonic negative MR has been found in (Bi,Pb)-Sr-Co-O, Bi-Ca-Co-O up to 9 T<sup>4,5</sup> and Ca<sub>3</sub>Co<sub>4</sub>O<sub>9</sub> up to 14 T.<sup>12</sup> (IV) The crystal with the  $x=0.3$  have the largest negative MR for all temperature except that above 12 T at 5 K. This is consistent with the data shown in Fig.2(a), where an intersection is observed at about 5.1 K of  $x=0.0$  and  $x=0.3$  MR curves. According to the susceptibility and  $\mu$ SR measurements,<sup>5,14</sup> the Pb-free crystal is almost paramagnetic down to 2 K. Ferromagnetism would be induced

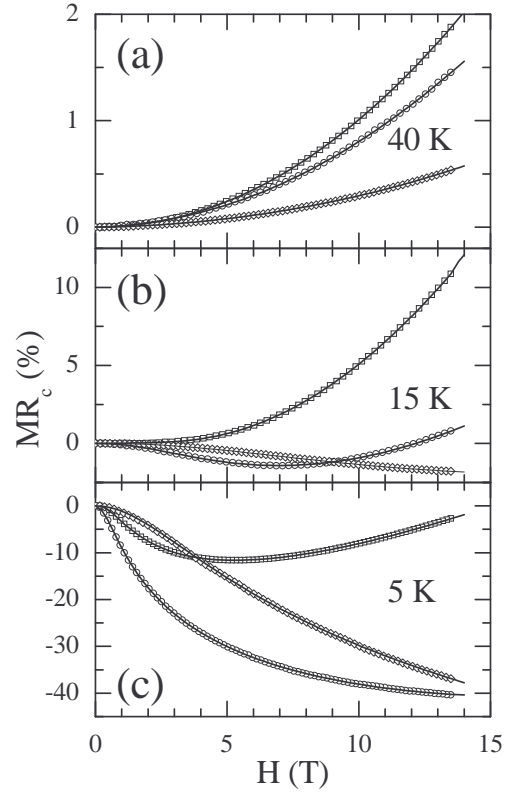


FIG. 5: The isothermal out-of-plane magnetoresistance as function of magnetic field at 40 K, 15 K, and 5 K for the samples with  $x=0.0$  ( $\diamond$ ),  $x=0.3$  ( $\circ$ ) and  $x=0.4$  ( $\square$ ). The subindex c of MR is referred to the out-of-plane configuration. The solid lines represent the data fitted by Eq. (1). The field is applied along c-axis.

by Pb doping and the transition temperature ( $T_c$ ) increases with increasing Pb doping level, with  $T_c=3.2$  K for  $x=0.44$  and 5 K for  $x=0.51$ , respectively. Thus in the present samples, the  $T_c$  is less than 3.2 K and beyond our measurement temperature range. The relative large magnitude of the negative MR at 15 K and 5 K may suggest the presence of short-range ferromagnetic correlation far above  $T_c$ .

In Fig. 4(b), the nonmonotonic field-dependence of MR is anomalous for triangular cobaltites, which has not been observed previously in these systems. Such a non-monotonic MR is more obvious in the out-of-plane MR. Figure 5 shows the evolution of the isothermal out-of-plane MR with magnetic field along c-axis at 5, 15, and 40 K for the three samples. The MR is positive at 40 K for all the samples (in contrast to the in-plane MR), and increases with increasing Pb doping level. The MR at 15 K is positive for  $x=0.4$ , while negative for the Pb-free crystal. These two samples exhibits monotonic MR at 15 K. On the contrary, the MR for  $x=0.3$  at 15 K is first negative and its magnitude increases with increasing magnetic field, and reaches a maximum ( $\sim 1.43\%$ ) at about 6.9 T, then decreases and passes through zero at 12.5T. The MR at 5 K is negative for all the crystals.

TABLE I: Values of the parameters to fit MR with Eq. (1). The out-of-plane MR for  $x=0.4$  at 40 K can fitted only using the second term in Eq. (1).

	$T(K)$	$A_1$	$A_2$	$B_1$	$n$
$x=0.0$ in-plane	5	3.51	0.23216	0	0
	15	1.41197	0.09207	0.26845	1.19685
	40	1.00262	0.05016	0.07236	1.59962
$x=0.0$ out-of-plane	5	3.57139	0.3064	0	0
	15	1.94482	0.10354	0.17494	1.66214
	40	0.61187	0.06884	0.07823	1.85638
$x=0.3$ in-plane	5	2.84001	0.73358	1.09044	0.77283
	15	2.78349	0.1563	0.39737	1.34744
	40	2.59917	0.03643	0.07917	1.65783
$x=0.3$ out-of-plane	5	2.78462	1.48822	0.29458	1.64505
	15	1.74818	0.23088	0.28285	1.77112
	40	0.42274	0.16466	0.13152	1.77808
$x=0.4$ in-plane	5	1.9198	0.62776	0.08762	2.19737
	15	1.6376	0.12996	0.17557	1.73868
	40	1.04661	0.049025	0.05667	1.45842
$x=0.4$ out-of-plane	5	2.50353	1.09468	1.24977	1.14875
	15	1.65991	0.22107	0.3908	1.81456
	40	0	0	0.09348	2.06279

The MR for  $x=0.0$  and  $0.3$  decreases monotonically with increasing  $H$ , while the MR of  $x=0.4$  exhibits an analogous behavior to that of  $x=0.3$  at 15 K, the magnitude of which first increases with enhancing  $H$ , and reaches a maximum ( $\sim 11.6\%$ ) around 5.3 T, then decreases. The above results are well consistent with the evolution of magnetoresistivity with  $T$  in Fig. 3. It should be pointed out that for the sample  $x=0.4$  the positive MR at 15 K is larger than that at 40 K, which is consistent with the hump observed in Fig. 3. The results above strongly suggest *the presence of a positive contribution in MR*.

Therefore, an expression consisting of negative and positive contributions for MR could be used to describe the anomalous nonmonotonic MR. It is found that all the isothermal MR can be well fitted by the following expression:

$$\frac{\Delta\rho}{\rho} = -A_1^2 \ln(1 + A_2^2 H^2) + B_1^2 H^n. \quad (1)$$

where  $A_1$ ,  $A_2$ ,  $B_1$ , and  $n$  are variable parameters for fitting. The fitted data are plotted in Fig. 4 and Fig. 5 by solid lines. All the isothermal MRs are well fitted. The fitting parameters are listed in Table I. The fitting parameters  $A_1$  and  $A_2$  increase with decreasing temperature.  $A_2$  is very small at 40 K, indicating that the negative contribution of MR is slight. For the out-of-plane MR of  $x=0.4$ , the first term is even zero. The  $A_1$  and  $A_2$  shows systematical temperature dependence, but no systematically concentration dependence is observed. Calculated with these values of  $A_1$  and  $A_2$ , the negative component of MR is the largest in magnitude for  $x=0.3$

at the three temperatures. Compared to  $A_1$  and  $A_2$ ,  $B_1$  and  $n$  varies more complexly. Neither systematical temperature dependence nor systematical carrier concentration dependence is found. For  $x=0.0$ , this term is absent at 5 K. At the other two temperatures,  $B_1$  is larger at 15 K and  $n$  is larger at 40 K. For the other two crystals, with decreasing  $T$ ,  $B_1$  increases, while  $n$  decreases, except in the in-plane case of  $x=0.4$ . For the in-plane MR of  $x=0.4$ , with decreasing  $T$ ,  $B_1$  decreases, while  $n$  increases. The calculated results for this term is rather complex. In the out-of-plane MR for  $x=0.3$ ,  $B_1$  decreases while  $n$  increases as the temperature is enhanced. While the calculated positive component is the largest at 15 K. In the out-of-plane MR for  $x=0.4$ ,  $B_1$  and  $n$  have the same evolution with temperature as that for  $x=0.4$ , while calculated positive component is the largest at 5 K. The increase of  $n$  enhances the dependence of the positive component on the magnetic field, while the decrease of  $B_1$  reduces it: they have the opposite effect on the positive component. This is the reason for the complex behavior of positive component of MR with temperature and carrier concentration. In general, the value of the positive component is relatively small at 40 K, and increases as the temperature decreases. This is consistent with the pronounced hump in the out-of-plane MR vs.  $T$  curves.

### C. The possible origin of the anomalous MR

#### 1. The negative component

The First term in Eq. (1) comes from a semiempirical expression proposed by Khosla and Fischer<sup>20</sup> and has been previously used to explain the negative MR observed in *n*-type CdS,<sup>20</sup> *n*-type Si<sup>21</sup> and (In,Mn)As.<sup>22</sup> The basis for this formula is Toyozawa's localized-magnetic-moment model of magnetoresistance, where carriers in an impurity band are scattered by the localized spin of impurity atoms.<sup>23</sup> It is derived from third-perturbation expansion of the *s-d* exchange Hamiltonian in this local-magnetic-moment model of Toyozawa.<sup>20,23</sup> Well agreement of the MR with the Eq. (1) reflects that the negative MR comes from the interaction between conducting carriers and localized magnetic moments, and it reveals a decrease of spin-dependent scattering of carriers in magnetic field. This model requires a separation of conducting carriers and localized magnetic moments. According to the photoemission and x-ray-absorption spectroscopy measurements in the misfit-layered (Bi,Pb)-Sr-Co-O,<sup>24</sup> both Co<sup>3+</sup> and Co<sup>4+</sup> have low spin configuration. The electrons of Co<sup>3+</sup> and Co<sup>4+</sup> locate in the  $t_{2g}$ , and the three-folded  $t_{2g}$  is split into one  $a_{1g}$  subband and two  $e'_g$  subbands due to the rhombohedral crystal field.<sup>27</sup> In Ref. 25, it has been pointed out that holes locate mainly in the  $a_{1g}$  subband, which are strongly coupled to the lattice and become localized holes. A minority of holes locate in the  $e'_g$  subbands. The former are "heavier" than the latter. The local magnetic moments are attributed to the  $a_{1g}$  holes<sup>5</sup> due to the strong electron-phonon coupling while  $e'_g$  holes is conducting carriers responsible for the relative low resistivity. Therefore, It is inferred that the conducting carriers formed by the  $e'_g$  holes interact with the localized magnetic moments from the  $a_{1g}$  holes through *s-d* exchange. Actually, such anomalous MR with nonmonotonic field dependence as shown in Fig. 5 has been previously observed in R<sub>2</sub>Ni<sub>2</sub>Si<sub>5</sub> (R=Pr, Dy, Ho, and Er) compounds, which was attributed to the presence of short-range ferromagnetic order in the literatures.<sup>25,26</sup> However, in the Pb-free crystal, it is reported to be paramagnetic down to 2 K.<sup>5,14</sup> Therefore, it seems to be difficult to be understood by the presence of short-range ferromagnetic order. Using Khosla-Fischer model with *s-d* exchange in localized-magnetic-moment model, the negative MR in these crystals may be well understood.

#### 2. Positive component

The hump feature in the out-of-plane MR vs *T* curves and the nonmonotonic isothermal MR strongly suggest the presence of the positive contribution in addition to the negative component. The second term in Eq. (1) gives the positive component of MR, which is proportional to  $H^n$ , with *n* varying from 0.77 to 2.19. The

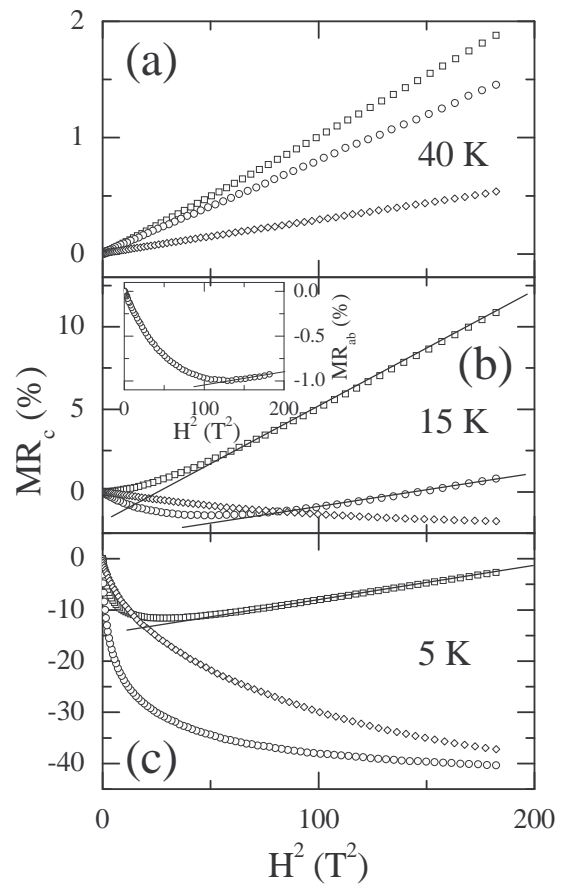


FIG. 6: The square magnetic dependence of the isothermal out-of-plane MR at 5, 15, and 40 K for the crystals with  $x=0.0$  ( $\diamond$ ),  $x=0.3$  ( $\circ$ ) and  $x=0.4$  ( $\square$ ). The inset shows the in-plane MR at 15 K for  $x=0.4$ . The field is applied along *c*-axis.

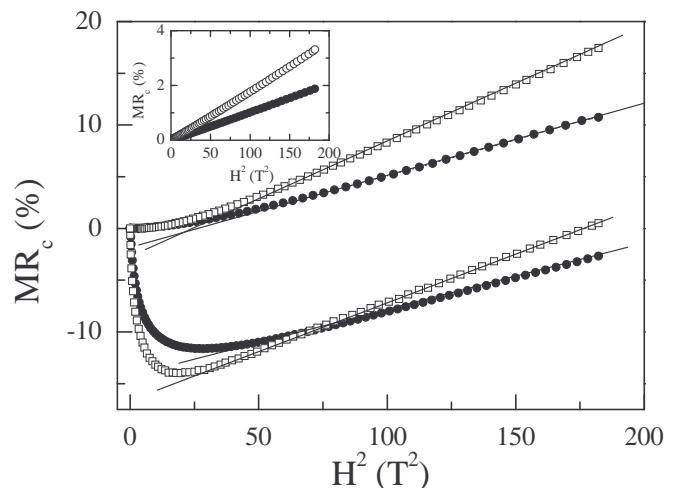


FIG. 7: The square magnetic field dependence of the isothermal transverse ( $\square$ ) and longitudinal ( $\bullet$ ) out-of-plane MR at 5, 15, and 40 K (the inset) for the crystal with  $x=0.4$ . Transverse and longitudinal configurations correspond to the field applied with *ab*-plane and along *c*-axis, respectively.

nonmonotonic MR found in  $R_2Ni_2Si_5$  ( $R=Pr, Dy, Ho,$  and  $Er$ ) is almost linear to  $H$  in high fields,<sup>25,26</sup> which is ascribed to the blocks structure.<sup>25</sup> While power law dependence of the positive component with power exponent dependent dramatically of  $T$  and sample is observed. In order to understand this behavior, the out-of-plane MR is plotted in Fig. 6 by  $H^2$  scales. It is intriguing that the upturn MR in high fields exhibits clear  $H^2$  behavior. In the inset of Fig. 6(b), the in-plane MR at 15 K for  $x=0.4$  also shows almost  $H^2$  behavior in high fields. It seems that in high fields the upturn MR is actually proportional to  $H^2$ . Large positive MR has ever been observed in  $Na_{0.75}CoO_2$  and  $[Bi_2Ba_{1.8}Co_{0.2}O_4]^{RS}[CoO_2]_2$ ,<sup>7,8</sup> and is proportional to  $H^2$  in the former, while nearly linear to  $H$  in the latter. The  $H^2$  dependence of positive MR in  $Na_{0.75}CoO_2$  was attributed to the conventional orbital motion of carriers.<sup>8</sup> However, this mechanism seems not to be plausible in the present samples. The increase of MR with decreasing temperature in  $Na_{0.75}CoO_2$  is accompanying with a dramatic enhancement in carrier mobility. However, in the present crystals, for example, for  $x=0.4$  the  $H^2$  behavior of the out-of-plane MR increases with decreasing  $T$  from 40 K to 15 K, while the semi-conducting resistivity suggests a reduction of mobility of carriers, and this is in contrast to the case in  $Na_{0.75}CoO_2$ . Furthermore, in classic Lorentz-force concept, the orbital motion of carriers would give no contribution to the longitudinal MR for spherical Fermi surfaces. Therefore, it suggests that detailed information of topology of Fermi surface is important to understand the observed magnetoresistive behavior. Fig. 7 shows the transverse and longitudinal out-of-plane MR plotted against  $H^2$ . The  $H^2$  dependence in high field can be clearly observed for all the curves. At each temperature, the transverse MR is larger than longitudinal one in high fields. It is interesting that the slopes of MR in high fields at 15 K and 40 K are almost the same in transverse or longitudinal case. This suggests that positive contribution saturates below 15 K. This positive contribution in MR is not understood yet. It may be associated with the complex magnetic structure in this system. Two possible magnetic configurations have been proposed by Yamamoto et al.,<sup>5,15</sup> (1)

A canted antiferromagnetic spin structure and (2) the co-existence of spin-glass and ferromagnetism, to interpret the weak ferromagnetism in Pb-doped crystals. In these two pictures, antiferromagnetic interaction is necessary. A positive MR with a slope following a  $H^2$  law can be expected for antiferromagnetic ordering.<sup>28</sup> The presence of AF interactions over the length of the mean free path would lead to a significant positive MR. More microscopic information and theoretical work are required to understand this anomalous nonmonotonic MR.

#### IV. CONCLUSION

We have observed an anomalous nonmonotonic field-dependent behavior of MR in (Bi,Pb)-Sr-Co-O single crystals. The MR exhibits a positive hump in high temperatures, following a negative behavior at low temperature, and the magnitude of the negative MR in low temperatures exhibits a maximum with magnetic field. These results strongly suggest that the MR comes from two contribution: one negative and one positive component. The *negative* component is described by the third-perturbation expansion of the  $s$ - $d$  exchange Hamiltonian in localized-magnetic-moment model of Toyozawa. The *positive* contribution follows a  $H^2$  law in high fields. The understanding of this anomalous nonmonotonic MR requires further experimental and theoretical work on the microscopic mechanisms.

#### V. ACKNOWLEDGEMENT

This work is supported by the grant from the Nature Science Foundation of China and by the Ministry of Science and Technology of China (Grant No. nkbrsf-g1999064601), the Knowledge Innovation Project of Chinese Academy of Sciences.

\* *Electronic address:* chenxh@ustc.edu.cn

<sup>1</sup> A. C. Masset, C. Michel, A. Maignan, M. Hervieu, O. Toulemonde, F. Studer, B. Raveau, and J. Hejtmanek, Phys. Rev. B **62**, 166 (2000).

<sup>2</sup> G. J. Xu, R. Funahashi, M. Shikano, I. Matsubara, and Y. Q. Zhou, Appl. Phys. Lett. **80**, 3760 (2002).

<sup>3</sup> D. Pelloquin, A. Maignan, S. Hebert, C. Martin, M. Hervieu, C. Michel, L. B. Wang and B. Raveau, Chem. Mater. **14**, 3100 (2002).

<sup>4</sup> A. Maignan, S. Hebert, M. Hervieu, C. Machel, D. Pelloquin and D. Khomskii, J. Phys: Condens. Matter **15**, 2711 (2003).

<sup>5</sup> T. Yamamoto, K. Uchinokura, and I. Tsukada, Phys. Rev. B **65**, 184434 (2002).

<sup>6</sup> S. Hebert, S. Lambert, D. Pelloquin and A. Maignan, Phys. Rev. B **64**, 172101 (2001).

<sup>7</sup> M. Hervieu, A. Maignan, C. Michel, V. Hardy, C. Creon, and B. Raveau, Phys. Rev. B **67**, 045112 (2003).

<sup>8</sup> T. Motohashi, R. Ueda, E. Naujalis, T. Tojo, I. Terasaki, T. Atake, M. Karppinen, and H. Yamauchi, Phys. Rev. B **67**, 064406 (2003).

<sup>9</sup> K. Takada, H. Sakurai, E. Takayama-Muromachi, F. Izumi, R. A. Dilanian, and T. Sasaki, Nature **422**, 53 (2003).

<sup>10</sup> M. L. Foo, Y. Y. Wang, S. Watauchi, H. W. Zandbergen, T. He, R. J. Cava, and N. P. Ong, Phys. Rev. Lett. **92**, 247001 (2004).

- <sup>11</sup> Y. Y. Wang, N. S. Rogado, R. J. Cava, and N. P. Ong, *Nature* **423**, 425 (2003).
- <sup>12</sup> X. G. Luo, X. H. Chen, G. Y. Wang, C. H. Wang, Y. M. Xiong, H. B. Song, H. Li, and X. X. Lu, cond-mat/0412298.
- <sup>13</sup> H. Leligny, D. Grebille, O. Perez, A. C. Masset, M. Hervieu, C. Michel, and B. Raveau, *C. R. Sci. Paris IIc, Chim* **2**, 409 (1999); *Acta Crystallogr., Sect. B: Struct. Sci.* **56**, 173 (2000).
- <sup>14</sup> J. Sugiyama, J. H. Brewer, E. J. Ansaldo, H. Itahara, T. Tani, M. Mikami, Y. Mori, T. Sasaki, S. Hebert, and A. Maignan, *Phys. Rev. Lett.* **92**, 17602 (2004).
- <sup>15</sup> I. Tsukada, T. Yamamoto, M. Takagi, and T. Tsubone, *Jpn. J. Appl. Phys.* **39**, 6658 (2000).
- <sup>16</sup> C. H. Wang, L. Huang, L. Wang, Y. Peng, X. G. Luo, Y. M. Xiong, and X. H. Chen, *Supercond. Sci. Technol.* **17**, 469 (2004).
- <sup>17</sup> T. Valla, P. D. Johnson, Z. Yusof, B. Wells, Q. Li, S. M. Loureiro, R. J. Cava, M. Mikami, Y. Morik, M. Yoshimura, and T. Sasaki, *Nature* **417**, 627 (2002).
- <sup>18</sup> T. Itoh, and I. Terasaki, *Jpn. J. Appl. Phys.* **39**, 6658 (2000).
- <sup>19</sup> T. Yamamoto, I. Tsukada, M. Takagi, T. Tsubone, and K. Uchinokura, *J. Magn. Magn. Mater.* **226-230**, 2031 (2001).
- <sup>20</sup> R. P. Khosla, and J. R. Fischer, *Phys. Rev. B* **2**, 4084 (1970).
- <sup>21</sup> R. P. Khosla, and J. R. Fischer, *Phys. Rev. B* **6**, 4073 (1972).
- <sup>22</sup> S. J. May, A. J. Blattner, and B. W. Wessels, *Phys. Rev. B* **70**, 073303 (2004).
- <sup>23</sup> Y. Toyazawa, *J. Phys. Soc. Jpn.* **17**, 986 (1962).
- <sup>24</sup> T. Mizokawa, L. H. Tjeng, P. G. Schultze, G. A. Sawatzky, N. B. Brooks, I. Tsukada, T. Yamamoto and K. Uchinokura, *Phys. Rev. B* **64**, 115104 (2001).
- <sup>25</sup> C. Mazumda, A. K. Nigam, R. Nagarajan, L. C. Gupta, C. Godart, G. Chandra, and R. Vijayaraghavan, *Phys. Rev. B* , 6069 (1996).
- <sup>26</sup> C. Mazumda, R. Nagarajan, A. K. Nigam, K. Ghosh, S. Ramakrishnan, L. C. Gupta, and B. D. Padalia, *Physica B* **339**, 216 (2003).
- <sup>27</sup> D. J. Singh, *Phys. Rev. B* **61**, 13397 (2000).
- <sup>28</sup> H. Yamada, and S. Takada, *J. Phys. Soc. Jpn.* **34**, 51 (1973).